NASA/TM—2009-215651/PART1

Preliminary Axial Flow Turbine Design and Off-Design Performance Analysis Methods for Rotary Wing Aircraft Engines; I-Validation

Shu-cheng S. Chen
Glenn Research Center, Cleveland, Ohio

May 2009

NASA STI Program . . . in Profile

Since its founding, NASA has been dedicated to the advancement of aeronautics and space science. The NASA Scientific and Technical Information (STI) program plays a key part in helping NASA maintain this important role.

The NASA STI Program operates under the auspices of the Agency Chief Information Officer. It collects, organizes, provides for archiving, and disseminates NASA's STI. The NASA STI program provides access to the NASA Aeronautics and Space Database and its public interface, the NASA Technical Reports Server, thus providing one of the largest collections of aeronautical and space science STI in the world. Results are published in both non-NASA channels and by NASA in the NASA STI Report Series, which includes the following report types:

- TECHNICAL PUBLICATION. Reports of completed research or a major significant phase of research that present the results of NASA programs and include extensive data or theoretical analysis. Includes compilations of significant scientific and technical data and information deemed to be of continuing reference value. NASA counterpart of peer-reviewed formal professional papers but has less stringent limitations on manuscript length and extent of graphic presentations.

- TECHNICAL MEMORANDUM. Scientific and technical findings that are preliminary or of specialized interest, e.g., quick release reports, working papers, and bibliographies that contain minimal annotation. Does not contain extensive analysis.

- CONTRACTOR REPORT. Scientific and technical findings by NASA-sponsored contractors and grantees.

- CONFERENCE PUBLICATION. Collected papers from scientific and technical conferences, symposia, seminars, or other meetings sponsored or cosponsored by NASA.

- SPECIAL PUBLICATION. Scientific, technical, or historical information from NASA programs, projects, and missions, often concerned with subjects having substantial public interest.

- TECHNICAL TRANSLATION. English-language translations of foreign scientific and technical material pertinent to NASA's mission.

Specialized services also include creating custom thesauri, building customized databases, organizing and publishing research results.

For more information about the NASA STI program, see the following:

- Access the NASA STI program home page at *http://www.sti.nasa.gov*

- E-mail your question via the Internet to *help@sti.nasa.gov*

- Fax your question to the NASA STI Help Desk at 301–621–0134

- Telephone the NASA STI Help Desk at 301–621–0390

- Write to:
  NASA Center for AeroSpace Information (CASI)
  7115 Standard Drive
  Hanover, MD 21076–1320

NASA/TM—2009-215651/PART1

Preliminary Axial Flow Turbine Design and Off-Design Performance Analysis Methods for Rotary Wing Aircraft Engines; I-Validation

Shu-cheng S. Chen
Glenn Research Center, Cleveland, Ohio

Prepared for the
65th Annual Forum and Technology Display
sponsored by the American Helicopter Society
Grapevine, Texas, May 27–29, 2009

National Aeronautics and
Space Administration

Glenn Research Center
Cleveland, Ohio 44135

May 2009

Level of Review: This material has been technically reviewed by technical management.

Available from

NASA Center for Aerospace Information
7115 Standard Drive
Hanover, MD 21076–1320

National Technical Information Service
5285 Port Royal Road
Springfield, VA 22161

Available electronically at http://gltrs.grc.nasa.gov

Preliminary Axial Flow Turbine Design and Off-Design Performance Analysis Methods for Rotary Wing Aircraft Engines; I-Validation

Shu-cheng S. Chen
National Aeronautics and Space Administration
Glenn Research Center
Cleveland, Ohio 44135

Abstract

For the preliminary design and the off-design performance analysis of axial flow turbines, a pair of intermediate level-of-fidelity computer codes, TD2-2 (design; reference 1) and AXOD (off-design; reference 2), are being evaluated for use in turbine design and performance prediction of the modern high performance aircraft engines. TD2-2 employs a streamline curvature method for design, while AXOD approaches the flow analysis with an equal radius-height domain decomposition strategy. Both methods resolve only the flows in the annulus region while modeling the impact introduced by the blade rows. The mathematical formulations and derivations involved in both methods are documented in references 3, 4 (for TD2-2) and in reference 5 (for AXOD). The focus of this paper is to discuss the fundamental issues of applicability and compatibility of the two codes as a pair of companion pieces, to perform preliminary design and off-design analysis for modern aircraft engine turbines. Two validation cases for the design and the off-design prediction using TD2-2 and AXOD conducted on two existing high efficiency turbines, developed and tested in the NASA/GE Energy Efficient Engine (GE-E^3) Program, the High Pressure Turbine (HPT; two stages, air cooled) and the Low Pressure Turbine (LPT; five stages, un-cooled), are provided in support of the analysis and discussion presented in this paper.

1. Introduction

For the airbreathing propulsion system analysis, the NASA Glenn Research Center has previously invested in the development of several high level design and analysis computer codes for the turbines and the compressors of the aircraft engines. Amongst these are a pair of intermediate level-of-fidelity axial flow turbine codes, TD2-2 (design; (ref. 1)) and AXOD (off-design; (ref. 2)), originally developed based on the aircraft engine technology of the 1970's (as documented in (refs. 3 and 4) for TD2-2, and in (ref. 5) for AXOD), but subsequently modified and upgraded to suit the preliminary design and analysis purposes for the modern day axial flow, subsonic to transonic, engine turbines. Both codes are very well constructed with exceptional knowledge and expertise, and they have been extensively validated over a number (up to ten) of existing advanced axial turbines, designed and tested by either the industry or by NASA. The purpose of this paper is to describe, in principle, the methodologies and the modeling strategies currently applied in the two codes, and to discuss the issues of applicability and compatibility between the two as a pair of companion pieces, to be used in the aircraft engine turbine design and the off-design performance analysis.

The arrangement of this paper is the following: The principles of the methodology of the codes are discussed for their differences and similarities, followed by comparison of the current modeling strategies and the model closure issues of the two methods, to establish the consistency and the compatibility between the two codes. Lastly, an optimization procedure for the model closure is illustrated, and the resulting turbine performance predictions are presented and discussed through examples.

2. Methodologies

The principle of the preliminary level of design and analysis method is to resolve only the flows in the annulus region of the turbine while modeling the impact introduced by the presence of the turbine blade rows. The flow is treated as axisymmetrical and steady, and in the annulus regions the viscous terms are neglected. From these assumptions, a set of first principle equations: mass conservation, streamwise momentum conservation, angular momentum conservation, radial momentum conservation, and the energy conservation, are enforced. And in TD2-2 and AXOD, the cylindrical coordinate system is adopted. These equations are, respectively:

$$\omega = 2\pi \int_{r_1}^{r_2} \rho V_x r \, dr \tag{1}$$

where ω is the mass flow rate through the annulus area r_1 to r_2, and V_x is the axial flow velocity;

$$Y_S = \left(P_{t1s} - P_{t1}\right) / \left(P_{t1} - P_1\right) \tag{2a}$$

$$Y_R = \left(P'_{t2s} - P'_{t2}\right) / \left(P'_{t2} - P_2\right) \tag{2b}$$

where Y_S and Y_R are the streamwise total pressure loss coefficients for the stator and the rotor, respectively, P_{t1s} and P_{t1} are the ideal and the actual absolute total pressures at the stator exit; P'_{t2s} and P'_{t2} are the ideal and the actual relative total pressures at the rotor exit, and P_1 and P_2 are the static pressures at the stator and the rotor exits, respectively;

$$W = \left(V_{u2}U_2 - V_{u1}U_1\right) / GJ \tag{3}$$

where W is the specific work-extract from the rotor, U_1 and U_2 are the rotor blade velocities, V_{u1} and V_{u2} are the tangential (circumferential) flow velocities at the rotor inlet and at the exit respectively, and G and J are the usual unit conversion factors;

$$\frac{G}{\rho}\frac{dP}{dr} = \frac{V_u^2}{r} - \frac{V_m^2}{r_m}\cos\upsilon \tag{4}$$

where V_m is the meridional flow velocity, $1/r_m$ is the streamline curvature, and υ is the meridional streamline slope angle, to be defined later. This equation is also known as the radial equilibrium condition. The energy conservation is expressed as

$$T_{t0} - T_{t1} = 0 \tag{5a}$$

$$T_{t2} - T_{t1} = -\frac{W}{\overline{C_p}} \tag{5b}$$

where T_{t0} and T_{t1} are the absolute total temperatures at the stator inlet and the exit, and T_{t2} is the absolute total temperature at the rotor exit. $\overline{C_p}$ is the specific heat at constant pressure, averaged off the two

stations. Lastly, a set of supplementary velocity component equations are listed to complete the system. They are:

$$V_m = \sqrt{V_x^2 + V_r^2} \tag{6a}$$

$$V = \sqrt{V_m^2 + V_u^2} \tag{6b}$$

$$\beta = \tan^{-1}\left(V_u / V_x\right) \tag{6c}$$

$$\upsilon = \tan^{-1}\left(V_r / V_x\right) \tag{6d}$$

where V is the absolute total velocity, V_r is the radial component of the flow velocity, β is the tangential flow angle, and υ is the meridional streamline slope angle.

These equations are listed in (ref. 3), and their derivations can be found in a number of textbooks, for example (ref. 6).

TD2-2 divides the annulus flow region into a number of stream tubes, each with an equal fraction of the total mass flow rate, and solves the principal equations (equations (1) to (5)) faithfully within each stream tube as a set of linear system differential equations (from the derivatives of equations (2), (3), (4), and (5); see (ref. 4)), eventually integrating the mass flow rate (equation (1)) from r_1 to r_2 to match the mass flow rate in the same tube upstream. This solution procedure marches axially downstream from station to station.

AXOD subdivides the flow annulus region into a number of concentric cylindrical areas of equal radius height, and assumes all relevant aerodynamic properties and the thermodynamic properties (such as the flow velocities, the total pressures, the total temperatures, and the coefficients of specific heat, etc.) are discrete constants radially within a sector (a leading order approximation, i.e., a constant within the subdivided area, but varying discretely from area to area), representable by the values obtained at the centerline of the subdivided area (sector). This treatment simplifies the solution algorithm dramatically since only the variations among a few discrete points (from sector center to sector center) at each station need to be processed, instead of having to integrate formally the whole flow domain (with an infinite number of varying points). The flow field is solved sequentially, essentially to satisfy the same set of first principle equations as that applied in TD2-2. The deficiency, of course, is the presence of discrete approximation error in the solution obtained, which is considered as a numerical error, reducible by increasing the number of sectors employed. A more fundamental error, however, is that the mass conservation in AXOD cannot be realized from an upstream station to the downstream station within each subdivided area, but can only be enforced globally by summing up all the mass flow obtained from each sector and match that to the upstream total mass flow. Since the mass conservation is not withheld within the same area element from upstream to downstream, the momentum and the energy conservations, derived for the unit mass flow rate of a conserved mass flow, expressed by equations (2), (3), and (5), are not strictly valid, but are to be regarded as an approximation to the conservation laws with the presence of approximation (true) errors. However, as was discussed and illustrated in (ref. 5), this approximation error injected into each sector is generally small, and becomes negligible with regard to the annulus area averaged physical quantities.

3. Modeling Strategies and Model Closures

The governing equations (1) to (5) are not a closed set of equations unless the loss coefficients (represented by Y_S and Y_R of equations (2a) and (2b)) are properly specified. Specifying the loss mechanism and the loss coefficients constitute the primary modeling activity of the methodology discussed. TD2-2 and AXOD have two very different models and modeling strategies.

In TD2-2, the loss mechanism is the total pressure loss across a blade row from an upstream tube to the downstream tube, exactly as that expressed by equations (2a) and (2b). The coefficients of loss, Y_S and Y_R, are modeled in close form by a composite functional given in (ref. 1) as:

$$Y_S = a_1 \frac{|\tan\beta_{in} - \tan\beta_{ex}|}{a_4 + a_5 \cos\beta_{ex}} \tag{7a}$$

$$Y_R = a_1 \frac{|\tan\beta'_{in} - \tan\beta'_{ex}|}{a_4 + a_5 \cos\beta'_{ex}} \tag{7b}$$

$$a_1 = 0.057\,,\ a_4 = 1.0\,,\ a_5 = 1.5$$

β here is the tangential flow angle, defined in equation (6c). The subscript *in* stands for the inflow, the subscript *ex* stands for the exit flow. The superscript (') stands for quantity in the relative frame. The model constants a_1, a_4, a_5 are obtained via validation data-fit. The rationale for the selection of this particular function is discussed in (refs. 1 and 3), briefly, the numerator $|\tan\beta_{in} - \tan\beta_{ex}|$ is a tangential blade loading factor ($F_u / \rho V_x^2 t$, t is the blade to blade spacing) and the blade row loss is expected proportional to this quantity; the denominator $\cos\beta_{ex}$ is inversely proportional to the trailing edge flow blockage, and its loss contributed to the presence of the blade row is expected to be proportional to $1/\cos\beta_{ex}$. Although simple and compact, these functions of the loss coefficients have been applied with success over ten existing turbine designs, as was illustrated in (ref. 1), which would suggest that these functional proportionalities might have captured the leading order behavior of the blade row losses.

The loss modeling applied in AXOD is more sophisticated than that in TD2-2 which is seen to have only a single mechanism, although ultimately they are to achieve the same goal, which is to close the linear momentum variation. The loss model in AXOD consists of three separate mechanisms. Firstly, the stagnation region total pressure loss factor (*YA*), expressed as:

$$YA_S = \left[\left(\frac{P_{t0}}{P_0} \right)^{\frac{\gamma-1}{\gamma}} - \left(\frac{P_{t01}}{P_0} \right)^{\frac{\gamma-1}{\gamma}} \right] \Bigg/ \left(\frac{\gamma-1}{2} \right) M_0^2 \tag{8a}$$

$$YA_R = \left[\left(\frac{P'_{t1}}{P_1} \right)^{\frac{\gamma-1}{\gamma}} - \left(\frac{P'_{t12}}{P_1} \right)^{\frac{\gamma-1}{\gamma}} \right] \Bigg/ \left(\frac{\gamma-1}{2} \right) M_1'^2 \tag{8b}$$

here, 01 represents an interim state immediately after the stator inlet state 0; 12 represents the interim state immediately after the rotor inlet state of 1. The subscript *t* stands for the total quantities; the superscript (') is for the quantities in the relative frame (of rotor).

Secondly, the blade row kinetic energy loss coefficient (*YB*), expressed as:

$$1-YB_S=\left(\frac{T_{t1}-T_1}{T_{t1}}\right)\Bigg/\left(\frac{T_{t1}^{id}-T_1}{T_{t1}^{id}}\right) \tag{9a-1}$$

$$1-YB_R=\left(\frac{T_{t2}^{'}-T_2}{T_{t2}^{'}}\right)\Bigg/\left(\frac{T_{t2}^{'id}-T_2}{T_{t2}^{'id}}\right) \tag{9b-1}$$

The superscript *id* stands for the ideal quantities, and they are defined as:

$$T_{t1}^{id}/T_1=\left(P_{t1}^{id}/P_1\right)^{\frac{\gamma-1}{\gamma}}=\left(P_{t01}/P_1\right)^{\frac{\gamma-1}{\gamma}} \tag{9a-2}$$

$$T_{t2}^{'id}/T_2=\left(P_{t2}^{'id}/P_2\right)^{\frac{\gamma-1}{\gamma}}=\left(\left[P_{t12}^{'}\left(\frac{T_{t2}^{'}}{T_{t1}^{'}}\right)^{\frac{\gamma}{\gamma-1}}\right]\Bigg/P_2\right)^{\frac{\gamma-1}{\gamma}} \tag{9b-2}$$

T_t^{id} is the ideal total temperature at the stator discharge, where the flow is assumed isentropically expanded in the stator from the interim state of 01 to the state of 1; and $T_t^{'id}$ is the ideal relative total temperature at the rotor discharge, where the flow is assumed isentropically expanded in the rotor from the interim state 12 to the state of 2. In regarding the total temperatures (absolute for the stator, relative for the rotor) at discharge, we have:

$$T_{t1}=T_{t0} \tag{9a-3}$$

$$T_{t2}^{'}=T_{t1}^{'}+\left(U_2^2-U_1^2\right)\Big/2GJC_p \tag{9b-3}$$

here, U_1 and U_2 are the blade velocities at the rotor inlet and at the rotor discharge, respectively.

These equations can be derived from the texts in (ref. 5).

The third loss mechanism is a blade row trailing edge blockage (flow area) loss factor (*YC*), expressed simply as:

$$\omega=\rho V_x*A*\left(1-YC_S\right) \tag{10a}$$

$$\omega=\rho V_x^{'}*A*\left(1-YC_R\right) \tag{10b}$$

where $A=\pi(r_2^2-r_1^2)$ is the sector area of the annulus at discharge.

As stated, AXOD solves the system equations sequentially, the procedure is this:

(1) The interim state (01 for the stator, and 12 for the rotor) total pressure is calculated using equation (8), and the discharge total temperature, T_{t1} (or $T_{t2}^{'}$), is obtained through equation (9-3). From these, the P_{t1}^{id} (or the $P_{t2}^{'id}$) is calculated using equation (9-2).

(2) A starting value for P_{t1}^{id}/P_1 (or for $P_{t2}^{'id}/P_2$) is guessed (actually, that means P_1 is guessed) from the mass flow function as:

$$\omega\sqrt{T_{t1}}\Big/\left(P_{t1}^{id} * A\right) = M_1^{id}\sqrt{\frac{\gamma G}{R}} * \sqrt{\frac{T_{t1}^{id}}{T_1}} * \left(\frac{P_{t1}^{id}}{P_1}\right)^{-1} \tag{11}$$

where,

$$1 + \frac{\gamma - 1}{2}\left(M_1^{id}\right)^2 = \frac{T_{t1}^{id}}{T_1} \tag{12}$$

(3) Equation (9) (i.e., (9a), (9b), and (9c) together) is solved to obtain the static temperature T_1 (or T_2) at discharge.

(4) With the static and the total temperatures known, the flow velocity components (V_x, V_u, V_r) are calculated. And with the static pressure, temperature, and the velocities known, the sector mass flow rate ω is calculated using equation (10).

(5) The process now moves to the next sector and the steps (1), (3), and (5) are repeated, but with the static pressure at each successive sector now calculated from the radial equilibrium condition instead of from the mass flow function (of step (2)).

(6) The mass flow rate of each sector are summed, and compared to the upstream total mass flow rate for satisfying the continuity condition.

When continuity is not satisfied the iterative process starts, by successively adjusting the guessed P_{t1}^{id}/P_1 (or the $P_{t2}^{'id}/P_2$) incrementally between an upper bound and a lower bound, where the upper bound started from the value of the critical P_t^{id}/P and the lower bound started with the value of one, but successively replaced by the previously guessed (P_t^{id}/P)'s. From this, an updated P_t^{id}/P (and thus the static pressure P) is obtained. The process now goes back to step (3) above, until the mass flow rate satisfies the continuity condition from upstream.

Note that in AXOD the (T_t^{id}/T)'s are not actually being used, only the (P_t^{id})'s and the (P_t^{id}/P)'s are calculated and recorded (saved into arrays). All the (T_t^{id}/T)'s in the formula given here are to be converted into functions of the (P_t^{id}/P)'s according to equation (9-2) when in use. And note also, that the (P_t^{id})'s are the ideal total pressures at discharge, not to be confused with the actual discharge total pressures, the (P_t)'s.

3.1 Model Closure for AXOD

Again, the solution-seeking procedure cannot commence unless the loss coefficients *YA*, *YB*, *YC* are specified, and interestingly, in AXOD these coefficients have not been assigned. The rationale is that, as an off-design code, the closure of the model is expected to be done consistent with the design point performance obtained through a design analysis process, which is conducted by a design code such as

TD2-2. And thus the closure of the model should be done by matching to the design point performance indices obtained from the design process.

In AXOD the mechanisms for this matching process are as follow:

(1) The blade row kinetic energy loss mechanism directly impacts the ideal and the actual states of the energy content at discharge (as reflected in the values of T_t and T obtained). Thus either the efficiency (such as the total efficiency or the static efficiency) or alternatively the total-to-static temperature ratio, obtained at the design point of a design process, can be matched by adjusting YB (the blade row kinetic energy loss coefficient).

(2) At a given mass flow rate, the discharge area blockage loss directly affects the discharge flow velocity obtained, and thus it also affects the value of the static pressure at discharge. Thus, the total-to-static pressure ratio (or alternatively the blade-jet speed ratio) can be matched by adjusting *YC* (the blockage loss factor).

(3) The stagnation region total pressure loss factor (*YA*) affects the values of the $\left(P_t^{id}/P\right)$'s, the $\left(T_t^{id}/T\right)$'s, and ultimately the ω's, thus this loss mechanism affects compositely the total pressure, the static pressure, and the static temperature at discharge.

From the basic compressible flow thermodynamic relation of

$$\frac{P_t}{P}=\left(\frac{T_t}{T}\right)^{\frac{\gamma}{\gamma-1}} \tag{13}$$

consider in a given system T_t is constrained (determined), for example, T_t does not change across the stator as indicated by equation (9a-3) and T_t' is specified through equation (9b-3), thus knowing P and T would uniquely determine P_t. It appears that the loss mechanisms in AXOD are over-specified. However, as indicated, P and T are functions of (*YB*, *YA*) and (*YC*, *YA*) respectively, thus P_t is a function of all (*YA*, *YB*, *YC*). In other words, adjusting *YA* would simultaneously vary P_t, P, and T, while the three are constrained by equation (13). This is indicative of the nature that the matching between the two system solutions (from AXOD to, say TD2-2) cannot be done perfectly, but can only be done closely. Thus there is the need to specify an additional constraint as a measure of goodness of the match. We define this constraint to be

$$RMSE=\sqrt{\left[\left(\frac{P_t-P_t^d}{P_t^d}\right)^2+\left(\frac{T-T^d}{T^d}\right)^2+\left(\frac{P-P^d}{P^d}\right)^2\right]\Big/3}\ =\text{Min} \tag{14}$$

where the superscript *d* stands for the design point value obtained from the to-be-matched system. At any given *YA*, there is a corresponding set of (*YB*, *YC*) that produces a minimum *RMSE*; and only at a particular *YA*, can the absolute minimum of *RMSE* be reached. Thus three loss mechanisms are needed.

Clearly, when the Min is zero, the two solutions are perfectly consistent. But a more relaxed condition for the consistency between the two system solutions (at the design point) can be stated as when the *RMSE* reaches the absolute Min.

In practice, of course, it is not the P_t, P, and T that are matched, but rather the total-to-total pressure ratio, the total-to-static pressure ratio, and the total efficiency (standard performance indices reported by almost all turbine codes) are matched to those of the given design point performance indices.

3.2 Similarity Laws for the Loss Mechanisms

With equation (14), and the mechanisms provided for the matching, the model in AXOD can be said to be closed. However, this matching process would have to be conducted from sector to sector, blade row to blade row, and stage to stage, which makes the process itself impractical. To alleviate this problem, a set of functional proportionalities (similarity laws) are defined for *YA*, *YB*, and *YC*. They are:

For the stagnation region total pressure loss factor (at the design condition), we define

$$YA_S = 1 - \left(\cos\lambda_S\right)^{\exp} \tag{15a-1}$$

$$YA_R = 1 - \left(\cos\lambda_R\right)^{\exp} \tag{15b-1}$$

with

$$\lambda_S \propto |\tan\alpha_{in} - \tan\alpha_{ex}| \tag{15a-2}$$

$$\lambda_R \propto |\tan\alpha'_{in} - \tan\alpha'_{ex}| \tag{15b-2}$$

where, the λ's are the stagnation region streamline deflection angles, and are assumed to be proportional to the flow circulation strength $\Gamma/2\pi r V_x$ generated by the blade row, which works out to be exactly that expressed by equation (15-2). The superscript exp in equation (15-1) is the order of power (the exponent), which is chosen empirically as 4 for the negative flow incidences and 3 for the positive flow incidences (given in (ref. 2); the flow incidences will be explained more later.) The α'*s* are the inlet and the discharge blade angles.

For the blade row kinetic energy loss, *YB*, we define

$$YB_S \propto |\tan\alpha_{in} - \tan\alpha_{ex}| \tag{16a}$$

$$YB_R \propto |\tan\alpha'_{in} - \tan\alpha'_{ex}| \tag{16b}$$

The rationale for this functional proportionality is as discussed previously in the loss modeling for TD2-2.

Lastly, for the trailing edge blockage loss factor, we define (again, with the same rationale as that stated in TD2-2):

$$YC_S \propto 1/\left(\cos\alpha_{ex}\right) \tag{17a}$$

$$YC_R \propto 1/\left(\cos\alpha'_{ex}\right) \tag{17b}$$

With these functional proportionalities, the loss factors *YA*, *YB*, and *YC* can be automatically determined from sector to sector, and/or from blade row to blade row, and/or from stage to stage, so long as a single set of (*YA*, *YB*, *YC*) values are explicitly specified on the meanline sector of the first stator.

Note that the inlet blade angles α_{in} (stator), α'_{in} (rotor) and the discharge blade angles α_{ex} (stator), α'_{ex} (rotor) are used instead of the flow angles (the β's). The blade angles are part of the geometric definitions of the turbine that are the required inputs to AXOD. Thus they are directly accessible, and in fact are more appropriate to use than the flow angles in representing the blade row characteristic functions. When the flows in the turbine blade rows are strictly subsonic, it is common that a preliminary design (not the off-design analysis) process would regard the blade angles (α, α') to be equal to the flow angles (β, β').

Through these similarity laws, the functional dependency of the loss model of AXOD is seen consistent with that of TD2-2.

As an off-design code, AXOD is primarily executing at the off-design conditions. In which, the *YA*'s, the *YB*'s, and the *YC*'s are all treated as invariants, based on the assumption that these dimensionless loss factors are predominantly geometric dependent (which is also reflected by the similarity relations applied here, that the dependency is only to the blade angles). As long as it is the same turbine operating at off-design, these loss factors should remain unchanged. There is, however, an additional stagnation region total pressure loss contributed from the inflow incidence effect at the off-design operation. This additional loss is augmented onto the *YA*'s directly as:

$$YA_S^{OD} = 1 - \left[\cos\left(Id_S\right)\right]^{\exp} \tag{18a-1}$$

$$YA_R^{OD} = 1 - \left[\cos\left(Id_R\right)\right]^{\exp} \tag{18b-1}$$

where,

$$Id_S = I_S + \lambda_S = (\beta_{in} - \alpha_{in}) + \lambda_S \tag{18a-2}$$

$$Id_R = I_R + \lambda_R = (\beta'_{in} - \alpha'_{in}) + \lambda_R \tag{18b-2}$$

As noted, the β_{in}'*s* are the inflow angles, and the α_{in}'*s* are the inlet blade angles. $(\beta - \alpha)$ is the formal (by definition) inflow incidence angle *I*, however, the inflow-incidences reported by AXOD are actually the *Id*'s.

With that, the modeling in AXOD is formally closed.

4. Results and Discussion

As illustrated in (ref. 1 and 2), TD2-2 and AXOD have been extensively validated. Amongst these are two turbine designs of particular interest, the High Pressure Turbine (HPT; two stages, air cooled) and the Low Pressure Turbine (LPT; five stages, un-cooled), developed and tested in the NASA/GE Energy Efficiency Engine (GE-E^3) Program. This HPT is the only cooled turbine studied, and the LPT contains the most number of stages (more challenging for the validation purpose.) Another obvious reason is that they are a pair of functioning turbines developed for the same aircraft engine. Both cases are documented with sufficiently detailed information in the GE reports, (refs. 7 and 8), in regarding the geometry, performance characteristics, and the experimental test data obtained on the turbine-built. The current study utilizes, to the extent possible, the established validation results documented in (ref. 1) and (ref. 2).

Two subjects of study are conducted here using the HPT and the LPT designs. First, the determination of the loss modeling coefficients (the design point performance indices matching process) of AXOD are conducted on the actual turbines (GE designs), and on the hypothetically designed turbines using the design code TD2-2 (cloned designs that closely follow the actual turbine geometries and the

design point operating conditions), to establish the compatibility of the two codes as a pair of companion pieces. Secondly, the off-design performance predictions, using the matched loss coefficients from the actual GE turbine design-point performances and the matched loss coefficients from the TD2-2 turbine designs, are conducted and compared with each other, and with the reported experimental test data, to demonstrate the applicability of the two codes as a set of viable tools for the preliminary turbine design and analysis purposes for the aircraft engines.

4.1 Loss Coefficients Optimization Procedure

4.1.1 The HPT's

The overall design point performance indices of the GE-E^3–HPT (as reported in (ref. 7)) and that of the HPT-design performed by TD2-2 are tabulated in table 1. Again, the TD2-2 design is conducted by cloning closely to the actual GE design while operating under the same design point conditions, including estimating as closely as possible of the added coolant flows.

TABLE 1.—THE ACTUAL DESIGN POINT CHARACTERISTICS OF THE HPT'S

	Rating efficiency	Total-to-total P.R.	Total-to-static P.R.	Corrected flow
GE design	0.916	5.04	5.66	18.026
TD2-2 design	0.9404	4.896	5.423	18.026

Knowing the design point performance indices, the off-design code AXOD matches these performance indices at the design point operating condition, by adjusting the loss coefficients *YA*, *YB*, and *YC* through the similarity laws expressed by equations (15), (16), and (17), until a minimum *RMSE* defined by equation (14) is achieved, thereby closing the loss models.

The resulting design point performance characteristics obtained by AXOD on the GE-E^3-HPT and the TD2-2-HPT, using respectively the set of optimum loss coefficients obtained through the processes of matching, are tabulated in table 2 and listed herein for convenience and clarity. Table 2 is to be compared with table 1 for assessment of the goodness-of-match achieved.

TABLE 2.—THE OPTIMUM MATCHING OBTAINED ON THE HPT'S BY THE PROCESSES OF AXOD

	Rating efficiency	Total-to-total P.R.	Total-to-static P.R.	Corrected flow
GE design	0.9155	5.046	5.657	18.0259
TD2-2 design	0.9398	4.889	5.435	18.0259

The actual matching processes conducted are illustrated here in three tiers: First, a stagnation region streamline deflection angle (λ) is assigned, and a blade row efficiency (1-*YB*) is sequentially (with a constant increment) varied. At each (λ, 1-*YB*) combination, the blockage factor (1-*YC*) is varied sequentially (again with a suitable constant increment) to capture a Tier I minimum *RMSE*. This is illustrated in figure 1. Next, All Tier I minimums are collected and plotted against the sequentially varying blade row efficiency (1-*YB*), this process is repeated over a number of assigned stagnation streamline deflection angles to identify a series of Tier II minimum *RMSE*'s. This process is illustrated in figure 2. Lastly the Tier II minimums are plotted against the incrementally varying streamline deflection angles (λ's) to identify the absolute (Tier III) optimum *RMSE*, as illustrated by figure 3.

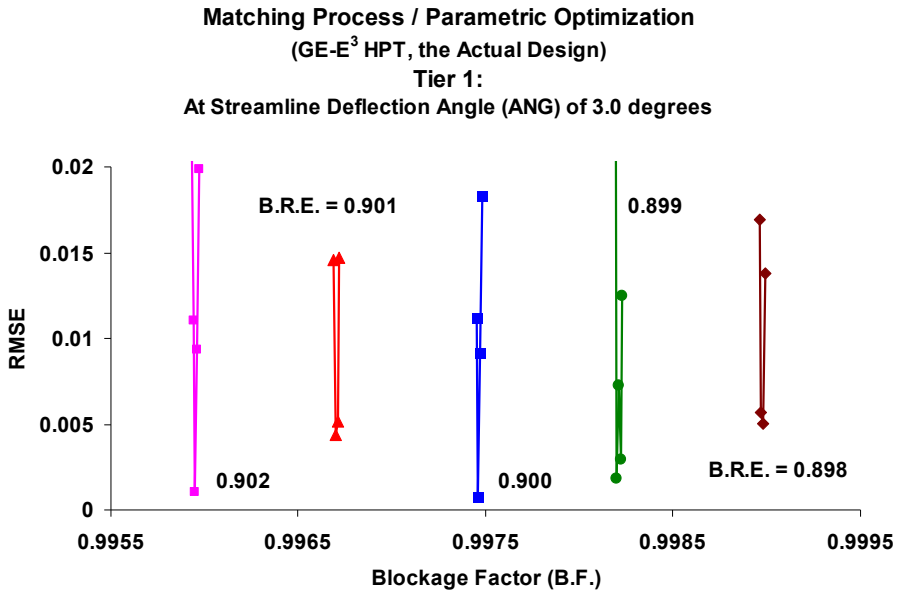

Figure 1.—Tier I Matching Process of the GE-E^3-HPT.

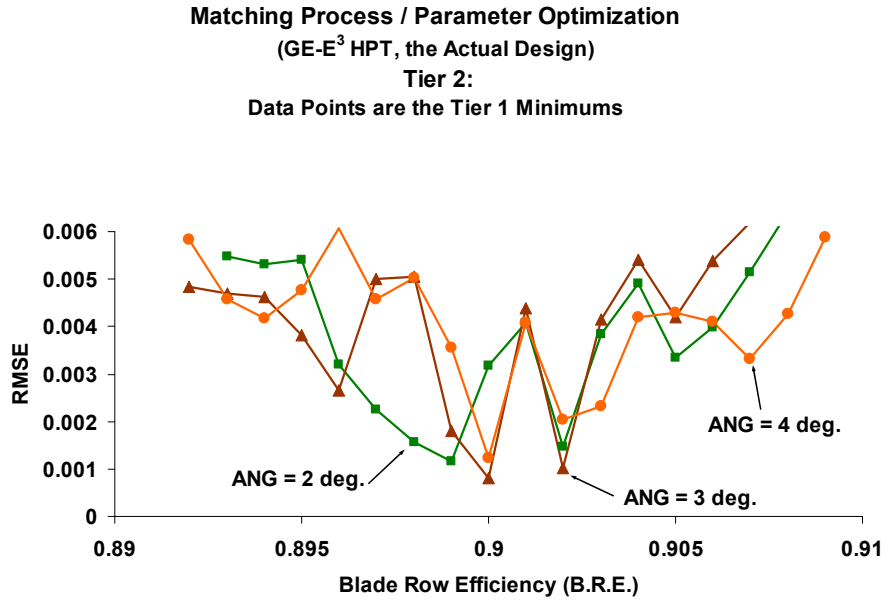

Figure 2.—Tier II Matching Process of the GE-E^3-HPT.

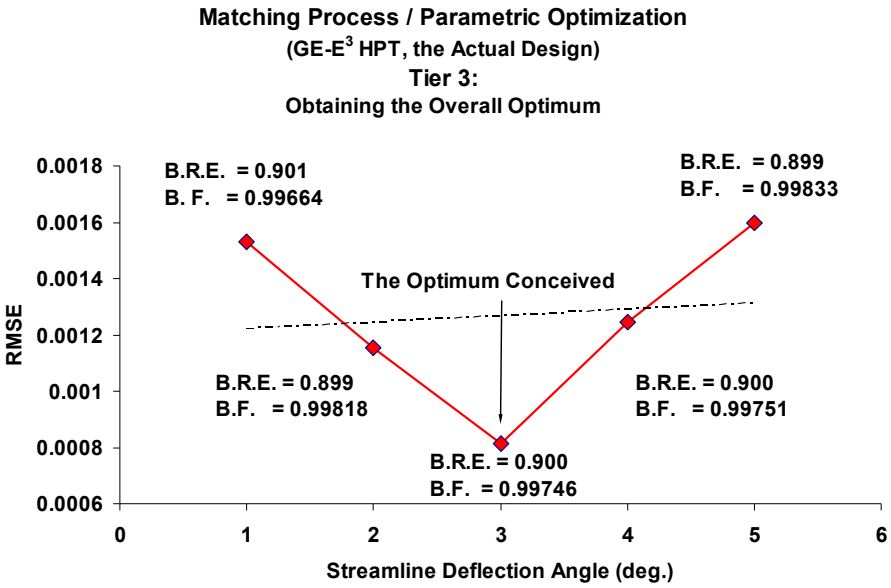

Figure 3.—Tier III Matching Process of the GE-E^3-HPT.

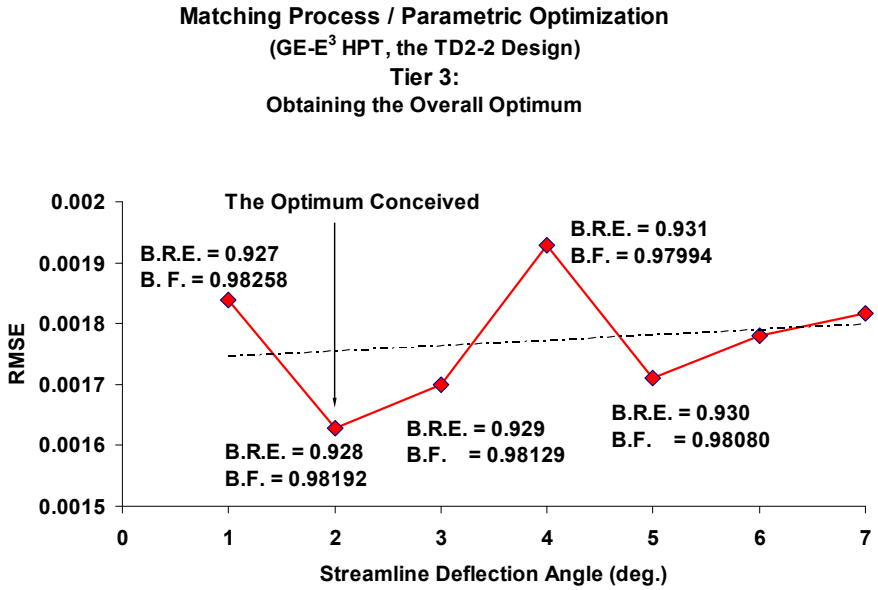

Figure 4.—Tier III Result of the Matching Process of the TD2-2-HPT.

The same tier-by-tier matching processes are conducted over the HPT of the TD2-2 design, but for simplicity, only the Tier III result is given here in figure 4.

The optimum loss parameters determined, respectively through these matching processes for the HPT's are listed in table 3. These are the set of parameters explicitly specified on the meanline sector of the first stator.

TABLE 3.—THE OPTIMUM LOSS PARAMETERS OBTAINED BY THE PROCESSES OF MATCHING ON THE HPT'S

	λ on the 1st stator, degrees	Blade row efficiency, 1-*YB*	Blockage factor, 1-*YC*
GE design	3.0	0.900	0.99746
TD2-2 design	2.0	0.928	0.98192

4.1.2 The LPT's

The same procedure is conducted on the LPT's. The overall design point performance indices of the GE-E^3–LPT (as reported in (ref. 8)) and that obtained from the LPT-design by TD2-2 are tabulated in table 4. Again, the TD2-2 design is conducted by cloning closely to the actual GE-E^3-LPT design while operating under the same design point conditions.

TABLE 4.—THE ACTUAL DESIGN POINT CHARACTERISTICS OF THE LPT'S

	Total efficiency	Total-to-total P.R.	Total-to-static P.R.	Corrected flow
GE design	0.920	4.37	4.76	38.08
TD2-2 design	0.9160	4.399	4.825	38.085

The off-design code AXOD matches these performance indices at the design point operating condition, by adjusting the loss coefficients *YA*, *YB*, and *YC* through the similarity laws expressed by equations (15), (16), and (17), until a minimum *RMSE* defined by equation (14) is achieved.

The resulting design point performance characteristics obtained by AXOD on the GE-E^3-LPT and the TD2-2-LPT, using the respective set of optimum loss coefficients obtained through the processes of matching, are tabulated in table 5. This table is to be compared with table 4 for the goodness-of-match, and is given here for clarity and for the ease of comparison.

TABLE 5.—THE OPTIMUM MATCHING OBTAINED ON THE LPT'S BY THE PROCESSES OF AXOD

	Total efficiency	Total-to-total P.R.	Total-to-static P.R.	Corrected flow
GE design	0.9201	4.378	4.753	38.085
TD2-2 design	0.9157	4.425	4.804	38.085

The same tier-by-tier matching processes are conducted over the LPT's. Again, these processes determine the optimum loss coefficients and the best match of the design point performance indices. For simplicity, only the Tier III results are given here. The Tier I and the Tier II plots of the GE-E^3-LPT are provided in the appendix as a reference.

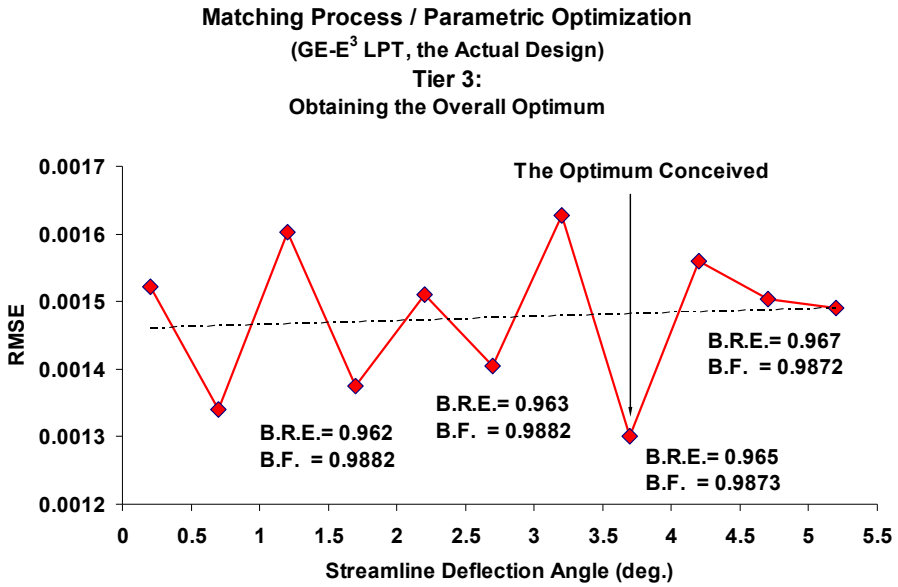

Figure 5.—Tier III Result of the Matching Process of the GE-E^3-LPT.

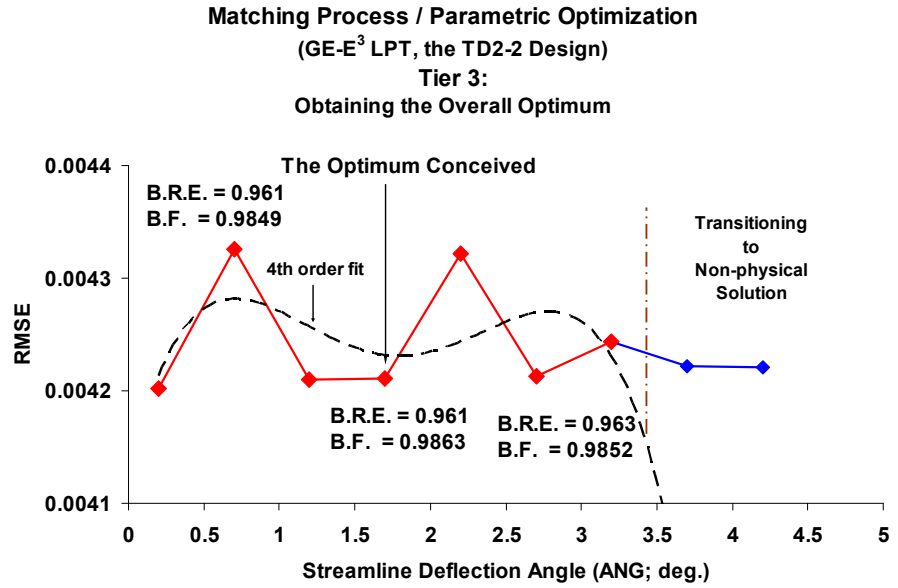

Figure 6.—Tier III Result of the Matching Process of the TD2-2-LPT.

The optimum loss parameters determined, respectively through these matching processes for the LPT's are listed in table 6. Again, these are the set of parameters assigned explicitly on the meanline sector of the first stator.

TABLE 6.—THE OPTIMUM LOSS PARAMETERS OBTAINED BY THE PROCESSES OF MATCHING ON THE LPT'S

	λ on the 1st stator, degrees	Blade row efficiency, 1-*YB*	Blockage factor, 1-*YC*
GE design	3.7	0.965	0.9873
TD2-2 design	1.7	0.961	0.9863

4.1.3 Remarks

Even with the similarity laws, where only one set of loss coefficients needs to be manually specified on the meanline sector of the first stator for each trial, the tier-by-tier optimization processes are still labor intensive and time consuming. Furthermore, the magnitude of the variation of the local optimums decreases from tier to tier. At Tier III, this difference in *RMSE* from point to point has deteriorated to nearly insignificant level, that the absolute optimum isn't apparent but has to be 'conceived', as can be observed from those Tier III plots. This suggests that the Tier III process, although mathematically plausible, is inaccurate and unreliable. Nevertheless, the Tier III process determines the *YA* (stagnation region total pressure loss) and as discussed in section 3 under Model Closure for AXOD, and also as indicated by the Tier III plots given here, a given *YA* (or equivalently, a given λ) changes the corresponding optimum values of (*YB*, *YC*). Thus, to simplify the optimization process, assigning a λ (the stagnation region streamline deflection angle) is practical and desirable, however, to preserve the physical significance of the losses obtained, this λ value should be assigned based on reasonable physical or mathematical observations. In (ref. 2), a λ of 6° is suggested for the HPT's (of any design) and a λ of 4° is suggested for the LPT's (of any design). Based on our Tier III plots, we would suggest to simply apply a λ of 3° for all turbines (HPT or LPT of any design). This assignment has been tested (with limited amount of cases, namely the cases under study in this work) and confirmed adequate.

4.2 Performances and Performance Validations

With the loss modeling closed and the optimum loss coefficients obtained, a series of off-design operations are calculated using AXOD on the HPT's and the LPT's of both the actual GE designs and the cloned TD2-2 designs. Results of these off-design performance predictions are plotted and compared with each other, and with the rig testing data reported by GE in (refs. 7 and 8). The experimental data reported are not easily convertible to the present form of dependent variables, the test data plotted here are adopted straight from the document of (ref. 2).

4.2.1 The HPT's

The performances of the HPT's operating at the off-design conditions are presented in figures 7 and 8.

Figure 7 shows the overall Rating Efficiency versus the overall total-to-static pressure ratio of the High Pressure Turbines, operating at three different rotational speeds. As shown, at off-design, the largest difference in the efficiencies predicted by AXOD using the two High Pressure Turbine designs (GE design and the cloned TD2-2 design) is within 3 percentage points, and either of the two efficiency predictions is within 1.5 points to the test data (the TD2-2 design over-predicts the efficiency).

Figure 8 shows the corrected mass flow rate versus the total-to-static pressure ratio. Note that the test data on flow rate plotted here has been scaled by a factor of (18.19/18.026), where 18.026 is the designed mass flow rate by the computer codes, and 18.19 is the reported rig test data of the mass flow rate at the design point condition. It would be fair to scale the test data accordingly so that the code prediction and the test result are consistent to each other at the design point. In figure 8, the largest difference between the predicted mass flow rates of the two turbine designs is in the negligible difference of 0.15 percent, and the largest difference between the code predictions and the test data is within 0.6 percent.

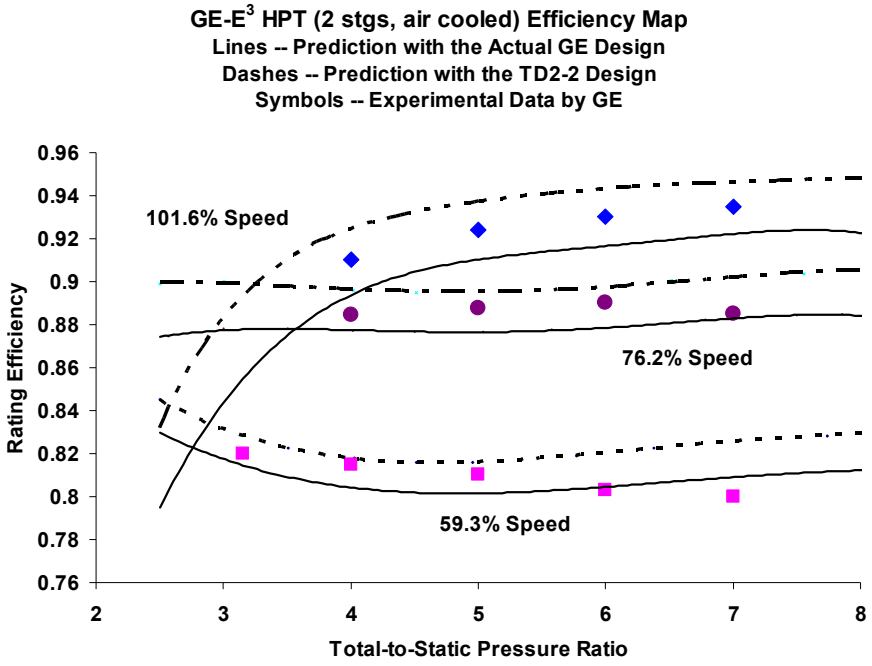

Figure 7.—Efficiency versus Pressure Ratio of the High Pressure Turbines at Various Rotational Speeds.

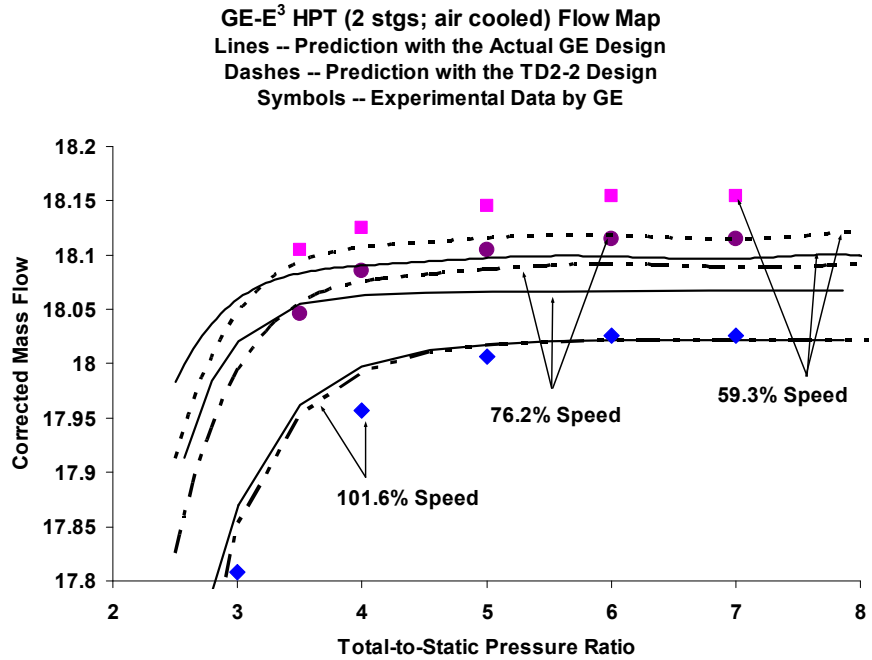

Figure 8.—Mass Flow Rate versus Pressure Ratio of the High Pressure Turbines at Various Rotational Speeds.

4.2.2 The LPT's

The performances of the LPT's operating at the off-design conditions are presented in figures 9 and 10.

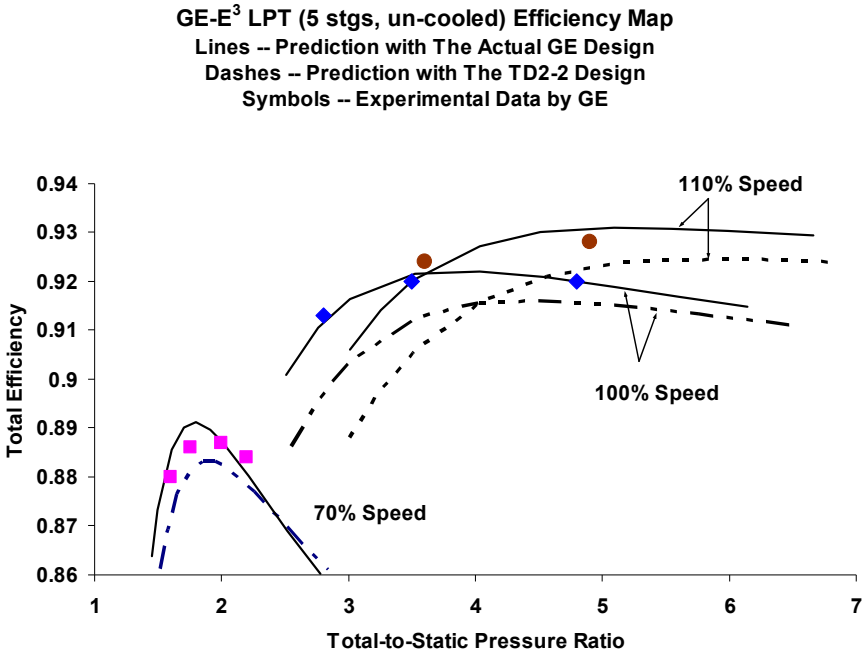

Figure 9.—Efficiency versus Pressure Ratio of the Low Pressure Turbines at Various Rotational Speeds.

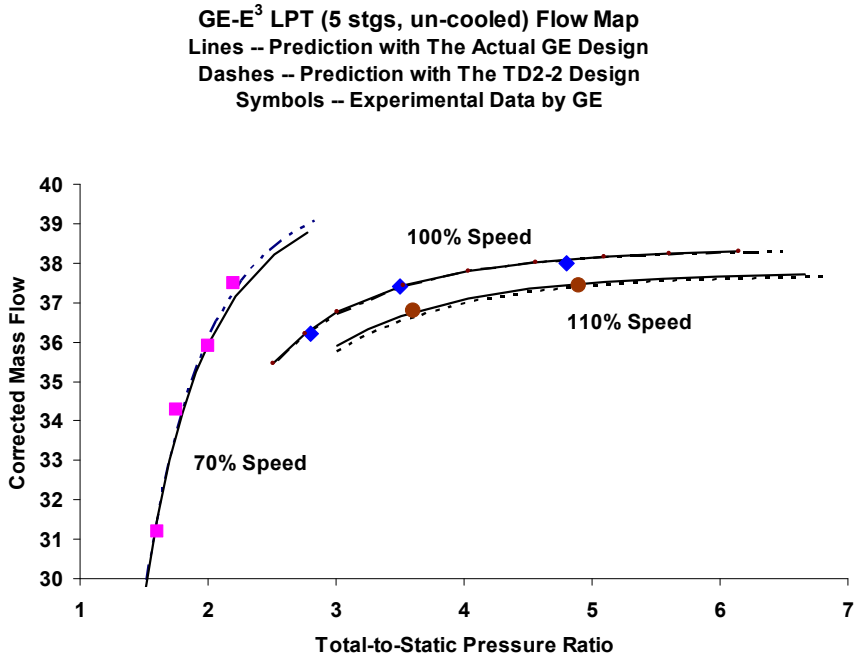

Figure 10.—Mass Flow Rate versus Pressure Ratio of the Low Pressure Turbines at Various Rotational Speeds.

Figure 9 shows the overall total efficiency versus the overall total-to-static pressure ratio of the Low Pressure Turbines, operating at three different speeds of rotation. As seen, at off-design, the predicted efficiency with the actual GE design virtually coincides with the reported test data. The largest difference in the efficiencies predicted by AXOD between the two Low Pressure Turbine designs (GE design and the cloned TD2-2 design) is within 2.5 percentage points (TD2-2 design under-predicts the efficiency at off-design conditions).

Figure 10 shows the overall corrected mass flow rate versus the overall total-to-static pressure ratio of the Low Pressure Turbines, operating at three different speeds of rotation. The difference between the predicted mass flow rates of the two turbine designs, and their comparison to the reported test data, are virtually indistinguishable.

Keep in mind that the TD2-2 designs are cloning the actual GE designs at the design point condition. At off-design operations, the cloned design would understandably perform differently than the actual design, from the latter were the test data acquired. In all, the off-design performances of the cloned turbine designs by TD2-2 are consistent and competitive to the performances predicted by the actual turbine designs, and both are compared favorably to the experimental data reported.

5. Concluding Remarks

The axial flow turbine design code (TD2-2) and the off-design performance analysis code (AXOD) were presented, compared, analyzed, and validated. The methodologies, the modeling strategies, and the model closures are shown to be consistent between the two codes. The off-design performances of the cloned turbine designs using the design code TD2-2 have been shown consistent and competitive to the performances predicted by using the actual turbine designs, and both are shown to compare favorably to the experimental data reported. This indicates that the design and the off-design codes (TD2-2 and AXOD) are fundamentally consistent and compatible to each other, and the methodologies applied are mathematically and physically sound. The work presented in this paper shows that these two codes can serve as a pair of companion pieces, to be used in the subsonic to transonic, axial flow turbine designs and off-design performance predictions for the modern aircraft engines.

References

1. "Users Manual and Modeling Improvements for Axial Turbine Design and Performance Computer Code TD2-2," Glassman, A.J., University of Toledo, NASA CR 189118, March 1992.
2. "Modeling Improvements and Users Manual for Axial-Flow Turbine Off-Design Computer Code AXOD," Glassman, A.J., University of Toledo, NASA CR 195370, August 1994.
3. "Analysis of Geometry and Design Point Performance of Axial Flow Turbines; I-Development of the Analysis Method and the Loss Coefficient Correlation," Carter, A., Platt, M., and Lenberr, F., NREC, Cambridge, MA, NASA CR-1181, September 1967.
4. "Analysis of Geometry and Design-Point Performance of Axial-Flow Turbines Using Specified Meridional Velocity Gradients," Carter, A. and Lenberr, F., NREC, Cambridge, MA, NASA CR-1456, December 1969.
5. "Analytical Procedure and Computer Program for Determining the Off-design Performance of Axial Flow Turbines," Flagg, E. E., General Electric Company, Cincinnati, OH, NASA CR-710, February 1967.
6. Turbine Design and Application; Volume I, Glassman, A.J., Editor, Lewis Research Center, NASA SP-290, 1972.
7. "Energy Efficient Engine High Pressure Turbine Component Test Performance Report," Timko, L.P., General Electric Company, Cincinnati, OH, NASA CR-168289, September 1990.
8. "NASA/GE Energy Efficient Engine Low Pressure Turbine Scaled Test Vehicle Performance Report," Bridgeman, M., Cherry, D., and Pedersen, J., General Electric Company, Evendale, OH, NASA CR-168290, July 1983.

Appendix

The Tier I and the Tier II plots of the parametric matching processes conducted on the GE-E^3-LPT design are provided here (figs. 11 and 12). The Tier III plot of this LPT design is shown by figure 5 in the main text. One observes that the Tier II plot here exhibits a smoother variation than the Tier II plot of the GE-E^3-HPT shown by figure 2.

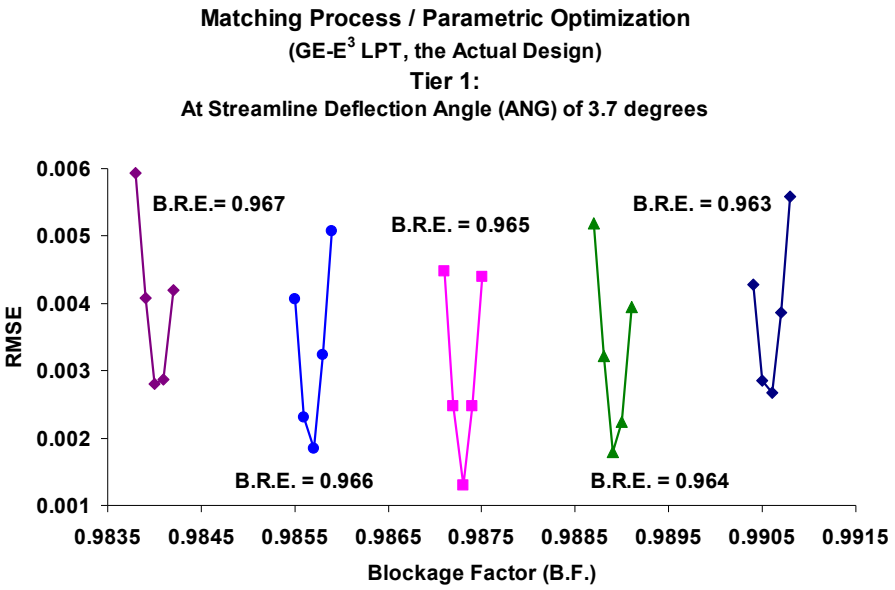

Figure 11.—Tier I Matching Process of the GE-E^3-LPT.

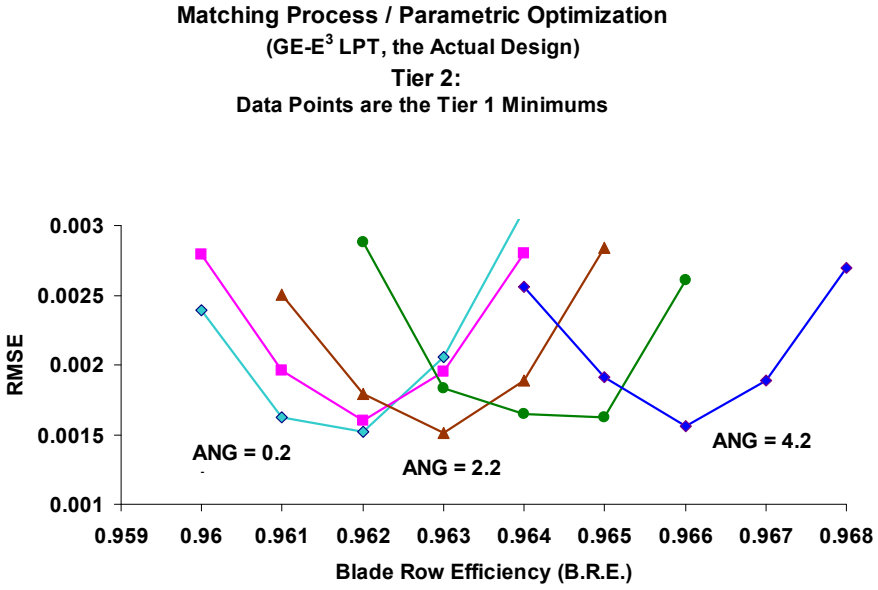

Figure 12.—Tier II Matching Process of the GE-E^3-LPT.

REPORT DOCUMENTATION PAGE	Form Approved OMB No. 0704-0188

1. REPORT DATE *(DD-MM-YYYY)*	2. REPORT TYPE	3. DATES COVERED *(From - To)*
01-05-2009	Technical Memorandum	

4. TITLE AND SUBTITLE
Preliminary Axial Flow Turbine Design and Off-Design Performance Analysis Methods for Rotary Wing Aircraft Engine; I-Validation

5a. CONTRACT NUMBER

5b. GRANT NUMBER

5c. PROGRAM ELEMENT NUMBER

6. AUTHOR(S)
Chen, Shu-cheng, S.

5d. PROJECT NUMBER

5e. TASK NUMBER

5f. WORK UNIT NUMBER
WBS 877868.02.07.03.01.02.02

7. PERFORMING ORGANIZATION NAME(S) AND ADDRESS(ES)
National Aeronautics and Space Administration
John H. Glenn Research Center at Lewis Field
Cleveland, Ohio 44135-3191

8. PERFORMING ORGANIZATION REPORT NUMBER
E-16964-1

9. SPONSORING/MONITORING AGENCY NAME(S) AND ADDRESS(ES)
National Aeronautics and Space Administration
Washington, DC 20546-0001

10. SPONSORING/MONITORS ACRONYM(S)
NASA

11. SPONSORING/MONITORING REPORT NUMBER
NASA/TM-2009-215651-PART1

12. DISTRIBUTION/AVAILABILITY STATEMENT
Unclassified-Unlimited
Subject Category: 07
Available electronically at http://gltrs.grc.nasa.gov
This publication is available from the NASA Center for AeroSpace Information, 301-621-0390

13. SUPPLEMENTARY NOTES

14. ABSTRACT
For the preliminary design and the off-design performance analysis of axial flow turbines, a pair of intermediate level-of-fidelity computer codes, TD2-2 (design) and AXOD (off-design), are being evaluated for use in turbine design and performance prediction of the modern high performance aircraft engines. TD2-2 employs a streamline curvature method for design, while AXOD approaches the flow analysis with an equal radius-height domain decomposition strategy. Both methods resolve only the flows in the annulus region while modeling the impact introduced by the blade rows. The mathematical formulations and derivations involved in both methods are documented in a series of NASA technical reports. The focus of this paper is to discuss the fundamental issues of applicability and compatibility of the two codes as a pair of companion pieces, to perform preliminary design and off-design analysis for modern aircraft engine turbines. Two validation cases for the design and the off-design prediction using TD2-2 and AXOD conducted on two existing high efficiency turbines, developed and tested in the NASA/GE Energy Efficient Engine (GE-E^3) Program, the High Pressure Turbine (HPT; two stages, air cooled) and the Low Pressure Turbine (LPT; five stages, un-cooled), are provided in support of the analysis and discussion presented in this paper.

15. SUBJECT TERMS
Axial flow turbines; Preliminary design and off-design analysis methods; Rotary wing aircraft engines

16. SECURITY CLASSIFICATION OF:			17. LIMITATION OF ABSTRACT	18. NUMBER OF PAGES	19a. NAME OF RESPONSIBLE PERSON
a. REPORT	b. ABSTRACT	c. THIS PAGE			STI Help Desk (email:help@sti.nasa.gov)
U	U	U	UU	25	19b. TELEPHONE NUMBER *(include area code)* 301-621-0390